

Low-loss austempered ductile iron gears: Experimental evaluation comparing materials and lubricants

Luis Magalhães, Ramiro Martins, Jorge Seabra

ABSTRACT

An experimental study to evaluate the power dissipation of gears was performed.

Three low-loss gear models were manufactured using standard 20° pressure angle tools. Austempered ductile iron (ADI) and 20MnCr5 carburized steel gears were tested in an FZG gear test machine using mineral, ester and polyalphaolephine (PAO)-based oils.

The results compare power dissipation, the influence of different tooth flank geometries, materials and lubricants.

This work concludes that conventional power-transmission gears can be replaced by these improved and more efficient low-loss models, which can be produced using common tools and that steel gears can be successfully replaced by austempered ductile iron gears.

Keywords:

Gears
Low-loss
ADI
Efficiency

1. Introduction

“Low-loss” refers to gears that are specially designed to operate with low friction between mating teeth. The amount of lost power can be significantly reduced by changing the tooth geometry of the gears [1–3]. New materials can replace steel, thereby improving the energetic efficiency of gears and gearboxes [4]. Being approximately 10% lighter than steel, austempered ductile iron (ADI) parts reduce power consumption in vehicles. It is shown in this work that ADI gears dissipate less power than steel gears in many operating conditions.

Since ductile iron began to be successfully austempered, years of development have produced several types of ADI strong enough to be used in gears. A copper–manganese ADI was produced for this work. This material was studied in previous work, showing that it can be safely used for gears. It has a noticeable resistance to scuffing, and its load-carrying capacity suggests its use in gears for mild-load applications [5–7].

This work compares the efficiency of ADI and steel low-loss gears operating at different speeds and loads, lubricated by different types of industrial oils. All the tests were performed using carburized 20MnCr5 steel and Cu–Mn ADI.

2. Low-loss geometry

The design of power transmission gears is usually done according to the expected mechanical resistance and operating life, and is generally based on bending stress at the tooth root and surface contact pressure. Once SN curves for pitting and fatigue resistance are established, a compromise between safety, gear geometry and expected operating life can be made. However, more efficient gears can be produced if low friction is the desired, assuring identical load-carrying capacity. This can simply be done by changing the geometric parameters of the gears (namely the shape and size of the teeth [1]).

Compared to standard gears, low-loss gears have many small teeth (see Fig. 1) that contact along very short paths, reducing friction. These gears must be helical to assure that contact is always occurring in more than one tooth pair. The face width is usually larger to increase the mechanical resistance of the small teeth. Their shape may be modified to increase tooth root resistance, namely increasing the working pressure angle of the gear.

The motion transmitted by a standard tooth pair is done by several small low-loss ones. This has dynamic consequences, as more contacts per time occur, reducing the critical resonance of the gear. In addition, the demands on the manufacturing quality are higher (of gears and gearbox elements), namely because the center distance tolerance becomes narrower as the gear module decreases. This limits the extent of reasonable modifications to increase power savings.

Three gear types were developed for this work (311, 411, 611). Gears 311 (70 teeth, 2.5 mm module, 20 mm width) were projected as low-loss equivalents to the type-C FZG spur gears (48 teeth, 4.5 mm module, 14 mm width). A balanced geometry was chosen for gears 411, allowing power loss savings without severe geometric modifications (75 teeth, 2.25 mm module). Type 611 was an advanced model, minimizing friction using 95 teeth (1.75 mm module) (see Table 1). All gears were helical (15°), and the teeth were 20 mm wide (face width). Manufacture followed general tolerance mk (ISO 2768) and quality class 6 (Q-DIN 3961).

The contact path length was reduced from 11.6 to approximately 5 mm, and the maximum sliding speed was decreased from 2.4 to 0.7 m/s (the wheel rotating at 1500 rpm). Reducing the approach and recess lengths (A–I and I–E, shown in Fig. 2) allows the teeth to engage/disengage at a lower relative speed (nearer to the pitch point), reducing friction. As a result, the oil bath is less heated, oil life increases and power loss is minimized. Thus, the low-loss geometry also reduces wear and the probability of scuffing, favoring a longer gear life. Fig. 2 compares the three gear types.

For simplicity, all the gears were manufactured using 20° rack tools and 15° helix angle (needed to assure suitable contact ratios). Positive profile shifts were used to provide similar mechanical resistance to the three gear types. (The safety coefficients were calculated according to DIN 3990 [8] and are shown in Table 2.)

3. Austempered ductile iron

Ductile iron (*spheroidal graphite iron*, *nodular iron*) requires substantially less processing than steel to be produced, and heat treatments are less energy-consuming. Ductile iron parts can be

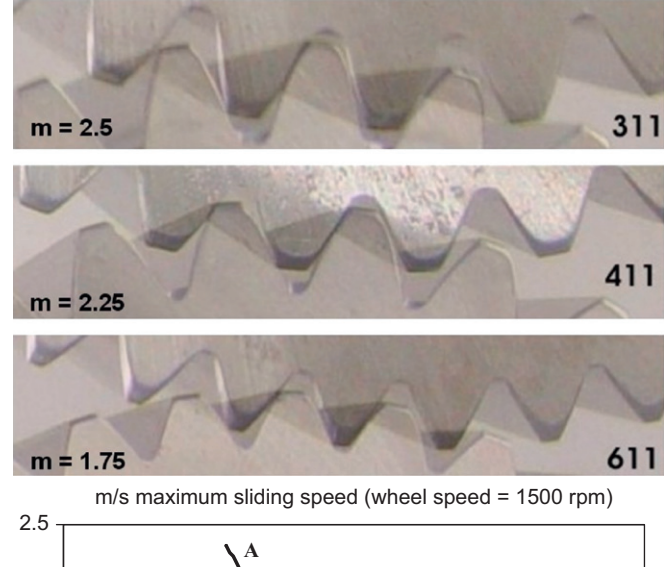


Fig. 2. Views of the pinion teeth of gears 311, 411 and 611 and the corresponding maximum sliding speed.



Fig. 1. FZG type-C gear (at the left) and equivalent low-loss gear (at the right) [2].

Table 1
Geometry of the low-loss gears developed for this work.

Gear parameters	Symbol	Unit	311		411		611	
			Pinion	Wheel	Pinion	Wheel	Pinion	Wheel
Module	m	mm	2.5		2.25		1.75	
Number of teeth	z	–	28	42	30	45	38	57
Working pressure angle	α_{wt}	deg		22.115		26.704		28.344
Addendum mod. coef.	x	–	0.1279	0.2500	0.9628	1.1500	1.7418	1.9500
Tip diameter	d_a	mm	78.047	114.892	77.504	113.287	76.406	111.558
Tip diam. mod. coef.	k	–		–0.031		–0.605		–1.018
Pitch diameter	d	mm	72.469	108.704	69.881	104.822	68.846	103.269
Working pitch diameter	d_w	mm	73.200	109.800	73.200	109.800	73.200	109.800
Transverse contact ratio	ϵ_{ps_a}	–		1.521		1.171		0.932
Overlap contact ratio	ϵ_{ps_b}	–		0.659		0.732		0.942
Total contact ratio	ϵ_{ps_t}	–		2.18		1.904		1.874
Contact path length	g	mm		11.575		8.022		4.966
Max. sliding speed ^a	v_{g_a}	m/s	2.175	2.371	1.710	1.441	1.242	0.708

^a At pinion and wheel tip, wheel speed = 1500 rpm.

Table 2

Safety coefficients and working parameters of the studied low-loss gears.

	Symbol	Unit	311		411		611	
			Steel	ADI	Steel	ADI	Steel	ADI
Safety coefficients								
Bending	SF	–	1.8	1.0	1.5	1.0	1.5	1.4
Pitting	SH	–	1.2	1.0	1.2	1.0	1.1	0.9
Scuffing	SB	–	3.5	2.58	4.21	2.96	–	–
Working parameters								
Hertzian pressure ^a	Po	GPa	1.17	0.97	1.19	1.01	1.29	1.11
Resonance speed	nE1	rpm	13,139	11,753	11,407	10,209	7778	6969
Gear friction power loss ^a	PVZ	kW	0.417	0.624	0.303	0.453	0.243	0.363

^a Speed = 1500 rpm, torque = 323 Nm (wheel). Transmitted power = 50.8 kW.

molded, while steel parts must be machined from previously laminated semi-products. Production costs can be significantly reduced, namely when machining gears, because the foundry parts only require finishing. In total, an ADI gear might cost 50% less than its high-resistance steel equivalent [9,10].

ADI is almost 10% lighter than steel, and its superior capacity to absorb vibration reduces noise from gearboxes. The high crack-propagation arrest ability of ADI inhibits sudden malfunctions that sometimes occur in very hard materials, namely carburized steel. However, ADI is not recommended for highly loaded gears because the graphite nodules near the surface might act as potential crack-initiation sites, eventually compromising the tooth bending resistance [6].

ADIs have characteristic surfaces on which a high number of small holes can be found, some still filled with graphite. This non-metallic phase determines the surface behavior, avoiding scuffing and providing lubrication under extreme working conditions, but ADI surfaces are not as smooth as steel ones, making the formation of very thin lubricant films difficult. These aspects are very important in determining the applications for ADI gears.

3.1. Copper–manganese ADI

Using ADI for power-transmission gears is only possible when improved iron alloys and heat treatments are selected. (Many low-resistant ADIs can be found, both in the literature and as daily products, in applications other than gears.) In addition, very different ADIs can be produced from the same ductile iron because the final properties depend on the austempering heat treatment. ADIs are classified into several grades by ASTM A897.

A die of Cu–Mn ductile iron was made to produce all the gears for this work. This 3.4%-C iron contains about 1% copper and 0.5% manganese (mass composition [11]) and was previously tested on gears with very good results [7]. Austempering aimed at a balanced ADI, without reaching too high of a mechanical resistance to avoid fragilization. Thus, after austenitization (875 °C, 40 min), the gears were isothermally transformed at 300 °C for 210 min. The average results (from tensile tests) were a rupture strength of 1313 MPa, yield strength of 1068 MPa and elongation ranging from 1% to 3%. Table 3 compares the properties of this ADI to 20MnCr5 carburized steel, both of which were used for the gears tested.

Several metallographic samples were prepared and evaluated to inspect the ADI quality. A good distribution of graphite was found inside a very close net of ferrite needles crossing the austenitic matrix (see Fig. 3). This microstructure is regular, compared to other ADIs, although the high density of ferrite needles resembles materials austempered at lower temperatures.

Table 3

Properties of carburized steel and ADI.

Units		20MnCr5	ADI ^a
Elastic module	GPa	210	153
Density	g/cm ³	7.85	7.06
Poisson's ration	–	0.3	0.25
Hardness	HRC	60	42
Tensile strength	N/mm ²	1300	1313
Yield strength	N/mm ²	850	1068
Elongation	%	8	2

^a Average tensile values measured from test specimen.

4. Lubricants

All gear tests were performed using a paraffinic mineral gear oil and then repeated using an ester and a polyalphaolephine (PAO) oil (see Table 4). These oils are fully formulated industrial gear oils, but the ester oil is less toxic than the others and is also biodegradable.

The PAO has a higher viscosity at all temperatures of approximately 5 cSt above the others at 100 °C (see Fig. 4), while the ester-based oil has significantly lower viscosity at 40 °C. In general, the oil viscosity increases the gear churning power losses. Simultaneously, a higher viscosity promotes a thicker lubricant film and a higher gear friction power loss if operating in full-film conditions. In mixed-film lubrication, a higher viscosity and higher film thickness might contribute to a slight reduction in the gear friction power loss. In any case, speed and load are the factors determining the choice of an adequate lubricant, in terms of power-loss.

Power transmission gears are commonly made of steel and lubricated with high-viscosity mineral oils. When high torques are transmitted, anti-wear (AW) and extreme-pressure (EP) additives are used to react with the steel working surfaces, forming compounds that avoid direct metal-to-metal contact. Some of these products are known to be toxic and harmful to the environment.

According to previous tests [5], Cu–Mn ADI performs well with base mineral oils, and the usual EP and AW additives do not seem to improve its performance. (The influence of graphite on the chemistry of AW and EP compounds is not yet clear, mainly due to the lack of available information on these products.) The performance of ester oil lubrication of ADI gears was evaluated in this work because, being biodegradable and non-toxic, this oil is not so harmful to the environment.

5. Efficiency tests

Tests were performed using a FZG machine (see Fig. 5). This well-known gear test rig was equipped with thermocouples

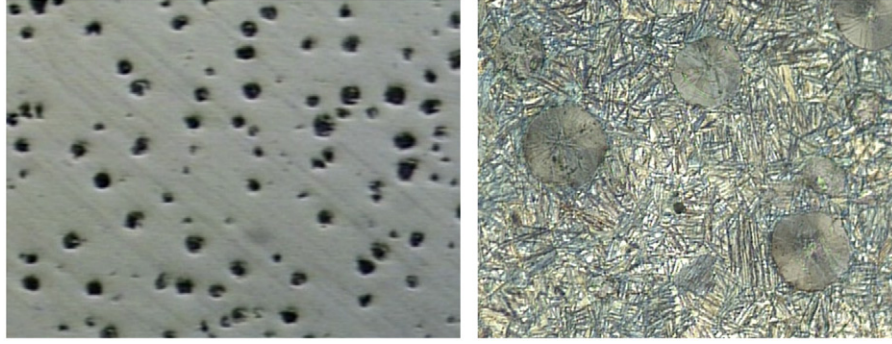


Fig. 3. Left: ADI surface ($\times 50$); and right: ADI microstructure ($\times 400$).

Table 4
Lubricant properties.

	Temperature ($^{\circ}\text{C}$)	Unit	Mineral	Ester	PAO
Density	15	ρ g/cm 3	0.897	0.925	0.848
Kinematic viscosity	40	ν_{40} cSt	146	99.4	151
Kinematic viscosity	100	ν_{100} cSt	14	14.6	19.4
ISO viscosity grade	–	VG	150	100	150
Viscosity index	–	VI	92	152	147
Piezoviscosity		α GPa $^{-1}$	9.7	11	14.3

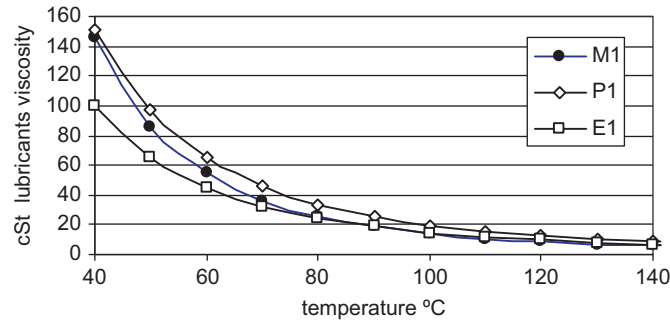


Fig. 4. Lubricant viscosities at different temperatures.

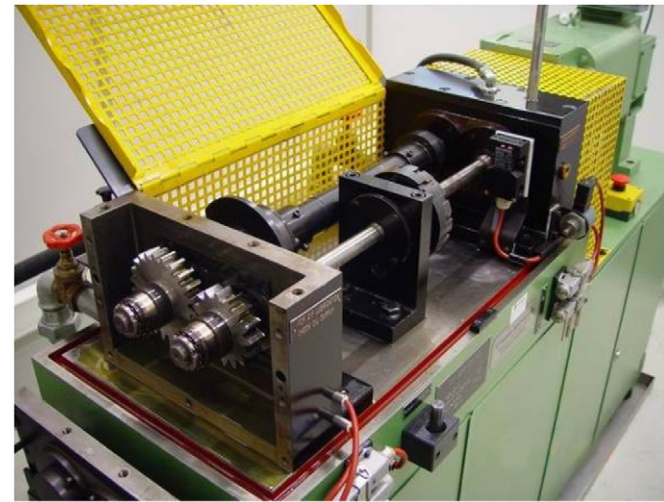


Fig. 5. Spur gear pair mounted in the FZG machine gearbox.

allowing continuous recording of the oil-bath temperature. The machine operated without lubricant cooling, allowing the temperature to rise freely during the tests.

Table 5
Loads and speeds at each test stage.

FZG load stage	Initial oil bath temperature($^{\circ}\text{C}$)	Wheel torque (Nm)	Wheel speed (rpm) and power (kW)		
			500	1000	2000
K1	Room	4.95	0.26	0.52	1.04
K5	40	104.97	5.50	11.00	21.99
K7	40	198.68	10.41	20.82	41.64
K9	40	323.26	16.93	33.87	67.74

All tests included a set of twelve 4 h stages, with each gear completing 3.36 million cycles. New steel and ADI gears were tested once for each lubricant and the lubricants were always replaced at the beginning of the tests. The test program included 3 gear types and 3 lubricants tested at 12 different combinations of speed and load.

Four load levels from the standard FZG-C pitting test and three rotational speeds were chosen (see Table 5). The first stage (K1) is almost a no-load situation with the power losses mainly depending on speed (500, 1000 and 2000 rpm). Load-dependent power losses become more important as the load is raised. At stage K9, these losses come mainly from gears and bearings.

Although the gears were designed to work under identical contact pressure, local conditions changed accordingly to test parameters, materials and lubricants. The specific lubricant film thickness was calculated for all the load stages of each test using average values of the working surface roughness and considering the temperature of the oil when steady-state operation was reached (see Section 6 for details). The friction coefficient was calculated according to Ref. [1] and the film thickness according to Ref. [12]. Lubrication regimes varied from mixed to boundary lubrication; thus, frequent metal-to-metal contact occurred. The combination of gear types and lubricants had a significant influence, with very thin films being created in load stage K9 and at 2000 rpm. Fig. 6 presents the minimum specific lubricant film thickness (λ) calculated for the steel gears at stage K9 (results are grouped by gear types [up] and by lubricants [down]).

Gears 311 worked with the lowest minimum film thickness regardless of the lubricant that was used. In order of increasing film thickness, the following trends were seen: 611-411-311 and ester-PAO-mineral (one exception for PAO-611). Comparing lubricants, the mineral oil and PAO allow for thicker films at a high torque and speed. However, ester has a much lower viscosity at low temperatures, and thus the churning losses can be considerably reduced when operating under such conditions.

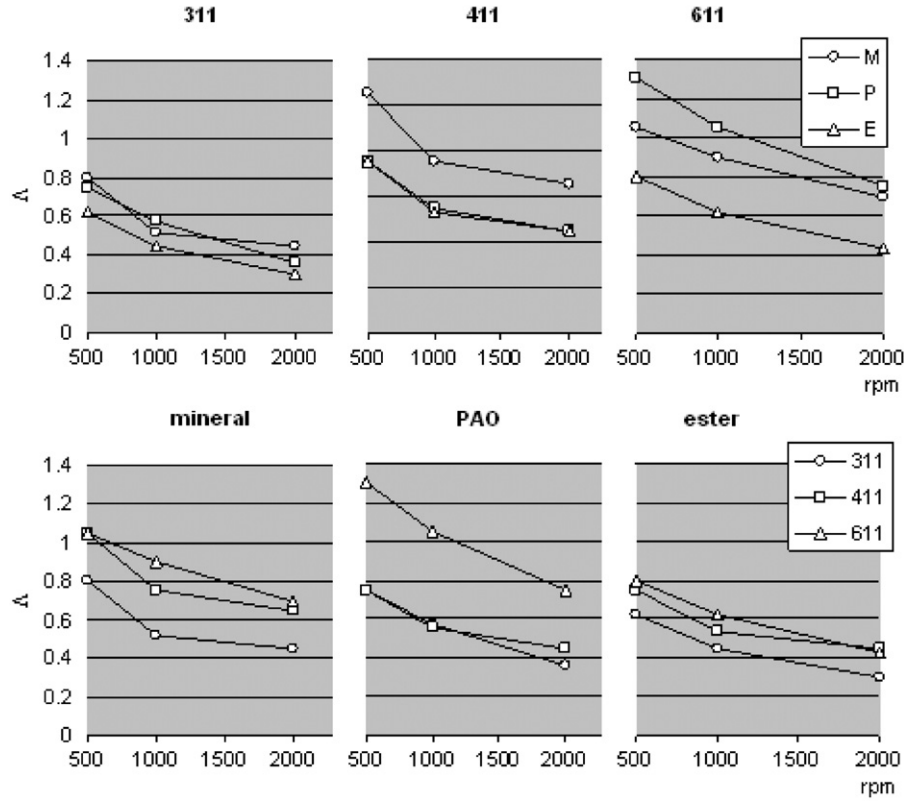


Fig. 6. Minimum specific lubricant film thickness (steel gears, K9 load level).

6. Power dissipation and heat balance

Gears, bearings and seals are the usual power loss sources inside the gearbox of the test rig. Churning (drag with the lubricant) is only speed-dependent at constant temperature, and the power loss in bearings and seals is also mainly speed-dependent under moderate loads. However, the load contribution to the power loss can be significant in loaded bearings, and the friction between gear teeth is mainly load-dependent (see Ref. [1] for details). The difficult task of separating the contribution of each heat source and to determine its dependence on load and speed requires a complex model that is under development [3].

An additional power-loss source was included in all the tests in this work because only a spur gearbox equipped with roller bearings having a low axial load capacity was available; a set of pressure pads was used to absorb loads resulting from the helical gears (this device transfers load from the pinion to the wheel and consists of a pair of discs mounted at the sides of the pinion—see Fig. 7). The contribution of the pads to the power loss was assumed to be the same in all tests performed under identical conditions.

It can be verified that an equilibrium temperature of the gearbox was attained after a certain operating time. In practice, when the sum of all heat sources matches the heat transferred by the gearbox to the environment (room air temperature may rise as friction heats the oil and the gearbox, mainly at the beginning of the tests, but after some hours of continuous operation, all temperatures tend to remain constant).

To compare the gears tested in this work, both the oil-bath and the room air temperatures were constantly recorded. The *stabilization temperature* (T_s) was defined as the difference between these temperatures, measured after 4 consecutive test hours. Because the operating conditions were the same in all tests, except for the gear geometry, the efficiency of the low-loss gear models was evaluated by comparing T_s in identical tests.

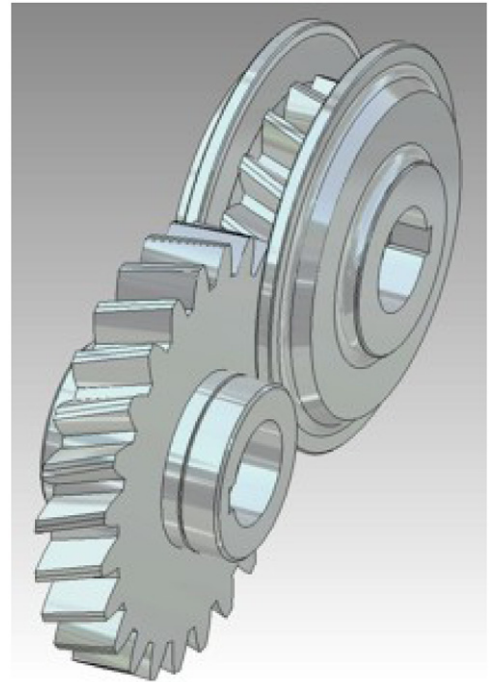


Fig. 7. Pressure pads mounted at the pinion sides.

7. Results

The stabilization temperature (T_s) was used to compare the gear efficiency (see Fig. 8). Globally, T_s increased by approximately 20 °C, wheel speed going from 500 to 1000 rpm and by approximately 40 °C, wheel speed going from 1000 to 2000 rpm.

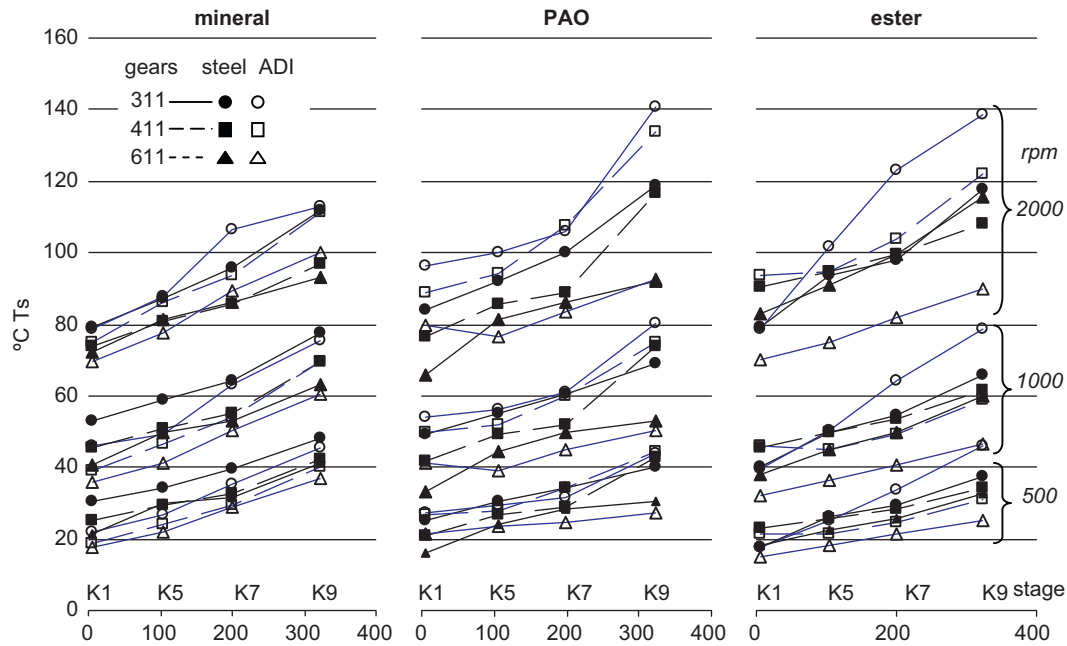


Fig. 8. Stabilization temperature (T_s) versus transmitted torque using three different lubricants (mineral, PAO and ester), three gear types (311, 411, 611) and two gear materials (white: ADI; black: steel).

Increasing the load from stage K1–K9 also increased T_s by approximately 20 °C at 500 rpm and by approximately 40 °C at 2000 rpm. T_s reached 140 °C in some tests, with the oil bath temperature rising to 160 °C.

The gears performed in the expected order: the 611 type was clearly more efficient than the 411 and 311 ones. Regardless of the lubricant, gears 611 performed better than the others. (The stabilization temperature at the end of the 611 tests was 10 °C to more than 40 °C lower.) This proves that the new low-loss gears can be very effective at improving the efficiency.

The ADI gears were, at the same time, the best and worst of all concerning efficiency (gears 611 and 311, respectively). This apparently contradicting behavior of ADI might be rationalized by considering the lubrication regimes that occurred at each specific test stage, depending on the teeth geometry and lubricants. The presence of graphite holes at the ADI surfaces does not allow thin lubricant films to be as stable as in steel, and oil additives interact differently with steel and ADI surfaces. Fig. 9 shows all T_s results grouped by lubricant, rolling speed and gear type.

In load stage K1, the stabilization temperatures of the ADI gears were generally lower than the temperatures of the steel gears when lubricated with mineral or ester oil. Conversely, the ADI performance using PAO oil was worse than steel under similar conditions. These results show that ADI and PAO did not work well together, even at low-load levels. Another important remark concerning the low-load stages is that the gear geometry was very influential in decreasing the stabilization temperatures at any speed, revealing that the new gears favor lower churning losses (as expected, this effect was more evident at 2000 rpm). Results also show that the increasing load from stage K1 to K9 caused a higher temperature increase in ADI than in steel, i.e., load-dependent power losses were generally higher using ADI.

Ester oil was generally better at low speeds and mineral oil at high speed and torque (with exceptions for some tests using the 611 gears). PAO oil was globally worse than ester, but better than mineral oil at low speed. Nevertheless, these results show that ADI can work well with all the lubricants tested, namely with the ester oil, whose lower viscosity at low temperatures might be a considerable advantage in terms of power loss.

In terms of absolute temperatures, only mineral oil withstood the power transmitted in stage K9 at 2000 rpm. PAO and ester oils did not work well with the 311 and 411 ADI gears under these conditions, but the 611 gears combined with ester oil achieved the best results. This fact is evidence of the high performance that the geometry of the new low-loss gears can provide.

Fig. 10 shows a plot of the difference between the steel and ADI stabilization temperatures in similar K1 and K9 tests ($T_{s\text{steel}} - T_{s\text{ADI}}$). Using mineral oil, steel performed better than ADI at 2000 rpm only. However, steel was better in almost all PAO tests, again with exceptions for the 611 gears. Ester oil favored the 311 steel gears at stage K9 and the 611 ADI gears at stages K1 and K9. The 411 gears confirmed the poor results for ADI using PAO oil and only favored ADI at lower speed tests using mineral and ester lubricants.

ADI performed better than steel using mineral and ester oils at low speed and load but not using the PAO lubricant. Using ester oil, the 611 ADI gears were clearly better than steel at all load levels and also better in most tests using mineral oil (with exceptions at 2000 rpm). Thus, ADI was more efficient than steel, mainly at lower speeds and also when the 611 gears were lubricated with ester oil. This opposite behavior might depend on the performance of the lubricant additives when reacting with steel or ADI.

8. Wear

The gears were weighed, and the roughness of the working surfaces of some teeth was measured before and after the tests. Oil samples were collected and analyzed to evaluate and quantify wear.

Graphite and void graphite holes play a complex role in the lubricant film formation mechanism, but inevitably they make the ADI surfaces much more uneven than the steel surfaces. Moreover, many small metallic particles are normally lost by ADIs during running-in, mainly due to the smoothing process of the edges of the graphite cavities [5].

Nodule cavities might be voided during gear manufacturing, or during gear testing, leaving several empty holes at the active flanks of the gear teeth. The depth and size of such holes

(reaching approximately 90 μm in diameter) can affect the surface roughness measurements and cause extreme measurements to be recorded. If an alignment of graphite holes is casually measured, the roughness parameters might not correctly represent the global contact surface. Thus, roughness measurements

must be carefully filtered in order to give a correct view of the graphite holes on ADI surfaces. Fig. 11 shows some profiles of the steel and ADI surfaces. (These were measured in very close locations of the same teeth before and after the tests.) It can be seen that deep valleys generated by the void graphite nodules remained in the ADI profiles, although the roughness of the working surfaces was strongly attenuated.

The steel surfaces were generally smoother than the ADI surfaces, with the Ra averaging 0.25 and 0.7 μm , respectively, while lowering to 0.2 and 0.5 μm after the test (attenuation of 20% for steel and 34% for ADI). These results accord with the mass-loss measurements, which were higher for ADI (see Fig. 12). Oil samples gathered during the tests were analyzed by ferrometry and analytical ferrography. The results of these tests showed that the ADI wear was more severe during all the test phases, consistently generating higher concentrations of wear debris and gradually contaminating the oil. Considering the higher roughness and the running-in mechanisms of ADI, these results were somehow expected.

A global trend of the 611 gears of lower wear is apparent, but exceptions occurred, namely, with the 311 steel gears and when the 611 ADI gear was lubricated by ester oil. (The PAO result for this gear is not available.) The influence of the gear geometry on the wear was much higher in ADI than in steel.

9. Discussion

The low-loss geometry of the new gears was constrained to a 20 mm face width, imposed by the use of pressure pads. Otherwise, it would be easy to reduce the contact pressure simply by enlarging the teeth, increasing the safety coefficients. The pads added an unknown load and speed-dependent power losses, thereby increasing the stabilization temperatures. Thus, the results of these tests may be compared with each other but not with results of any other tests that do not include the pressure pads.

The wear and mass loss were much higher using the ADI gears. However, the gears were all new (not run-in), and particles accumulated in the oil during the 12 stages of each test. Thus, the particle count includes both normal and running-in wear. (The oil was only replaced at the beginning of each test.) This fact must be taken into account because new ADI surfaces normally lose a very significant number of small particles during running-in.

Machine preparation, mounting and dismounting gears, testing, oil analysis and surface inspection are highly time-consuming. Although it is a large test program, the study only provided one result for each specific combination of materials, lubricants and

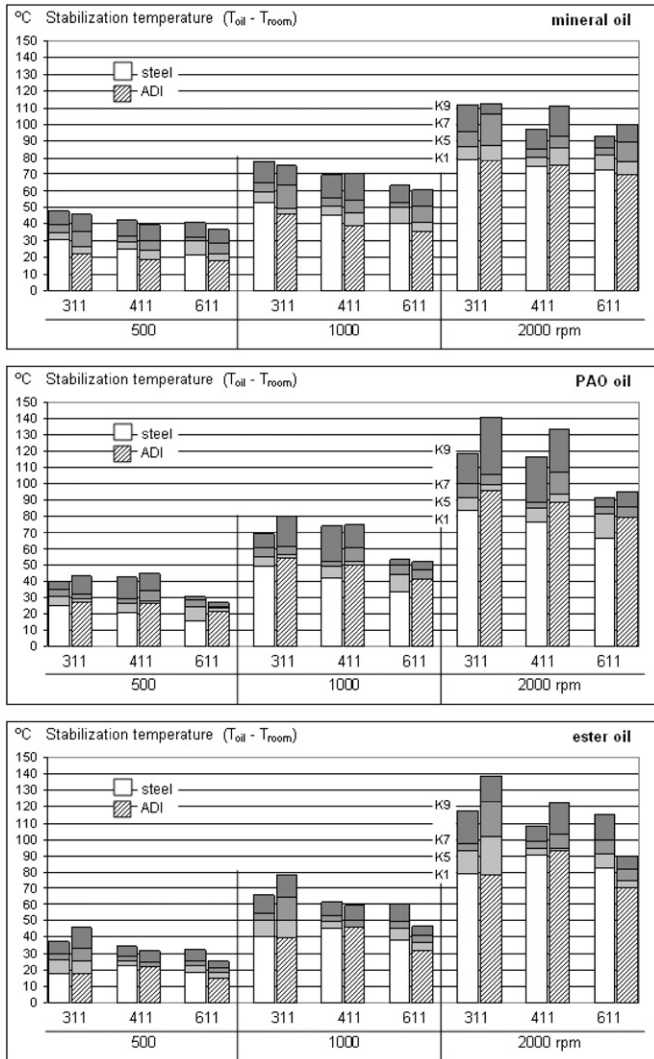


Fig. 9. Stabilization temperatures grouped by lubricant type.

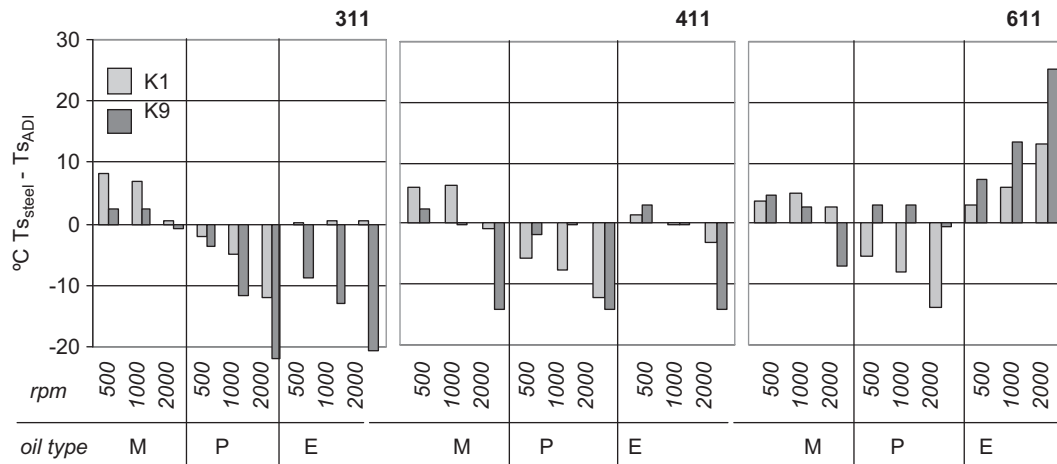


Fig. 10. Comparison of the steel and ADI stabilization temperatures at stages K1 and K9.

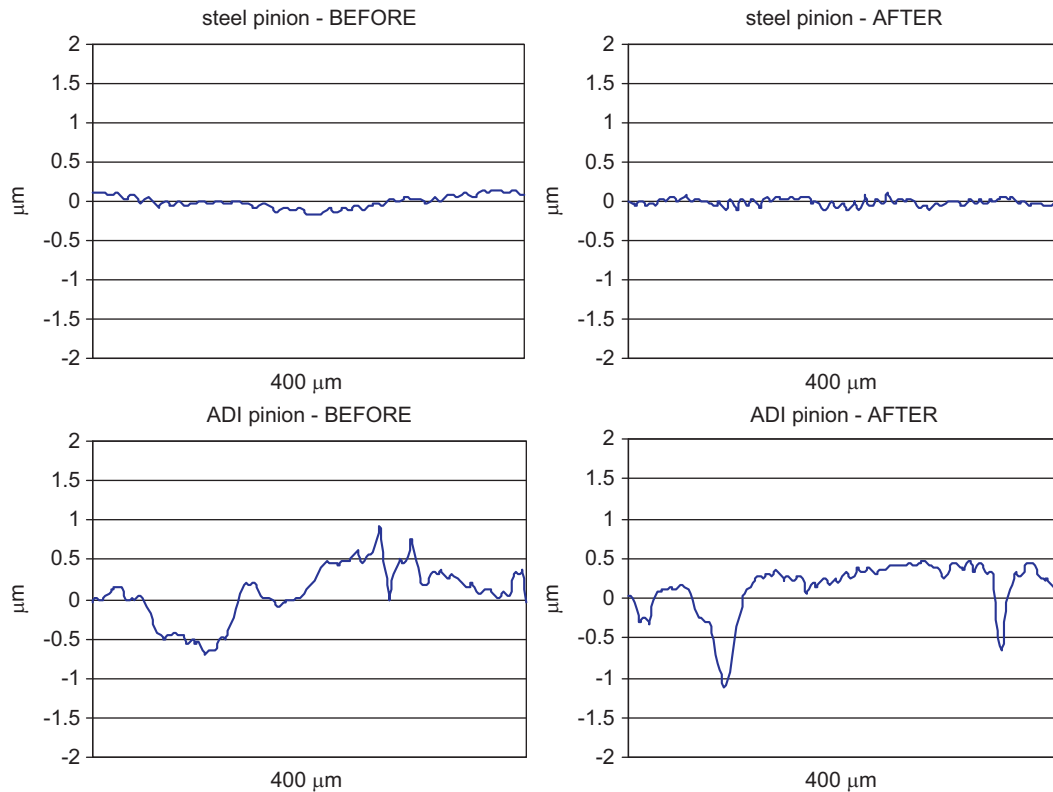


Fig. 11. Samples of the roughness profiles of the ADI and steel pinions before and after respective tests.

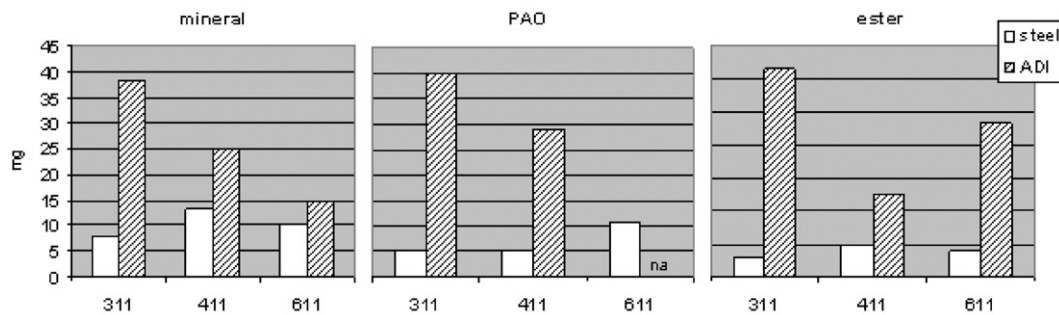


Fig. 12. Total mass loss of the steel and ADI gears.

operating conditions. Considering this fact, the results must not be seen as absolute and are more meaningful when considered globally or by item group and still require statistical validation.

10. Conclusions

The new gear geometries were very effective in reducing the power loss, and proportionality between the level of modification of the gears and the results was found. This finding proves that low-loss gears can be manufactured using common, standard 20° pressure-angle cutting tools, and that significant energy savings are obtained simply by changing the geometry of the tooth profiles.

Cu-Mn ADI gears performed very well, compared to carburized steel ones, and their efficiency was even better in many situations, particularly when the speed and load were not too high. However, the measured temperatures depended significantly on the lubricants. The ADI gears performed well using mineral and ester oils, but results using PAO were not so good. The 611 ADI gears were always more efficient than the steel gears

using ester oil, namely when transferring high torque. It may be concluded that a good combination of materials and lubricants depends on the operating conditions, namely on speed and load, which will determine the proportion of speed- and load-dependent power losses.

Wear was always higher for the ADI than for steel gears, which must be related to the surface properties and lubrication regimes. However, the low-loss geometry was found to reduce wear very favorably, and this effect was more noticeable for the ADI gears.

ADI was a good choice for replacing steel at moderate load and speed, conditions at which the ester oil significantly contributed to a decrease in the power loss, while mineral oil was generally better operating at high speed and load.

Acknowledgments

The authors thank FCT (*Fundação para a Ciência e Tecnologia*) for supporting the project “Low Power Loss ADI Gears” (PTDC/EME-PME/73389/2006).

References

- [1] Höhn BR, Michaelis K, Wimmer A. Low loss gears. *Gear Technology* 2007;24(4).
- [2] Michaelis K, Hohn B, Hinterstoißer M. Influence factors on gearbox power loss. *Industrial Lubrication and Tribology* 2011;63/1:46–55.
- [3] Magalhães L, Martins R, Locateli C, Seabra J. Influence of tooth profile on gear power loss. *Industrial Lubrication and Tribology* 2011;63/1:27–33.
- [4] Magalhães L, Martins R, Seabra J, Gonçalves R. Low Torque Loss Gears: Austempered Ductile Iron vs Carburized Steel. Lulea, Sweden: NORDTRIB; 2010.
- [5] Magalhães L, Seabra J. Wear and scuffing of austempered ductile iron gears. *Wear* 1997;215(237–246).
- [6] Magalhães L, Seabra J. Experimental observations of contact fatigue crack mechanisms for austempered ductile iron (ADI) discs. *Wear* 2000;246(134–148).
- [7] Martins R, Seabra J, Magalhães L. Austempered ductile iron (ADI) gears: power loss, pitting and micropitting. *Wear* 2008;264(838–849).
- [8] Standard DIN 3990. . Calculation of the Load Capacity of Spur and Helical Gears; 1987.
- [9] Harding, RA. The Use of Austempered Ductile Iron for Gears, 2^o World Gear Congress, Paris; 1986.
- [10] Ductile Iron Data for Design Engineers, Ductile Iron Society, Sorelmetal Technical Services, Rio Tinto Iron & Titanium Inc.; 1998.
- [11] Santos, H, Pinto A, Torres V. Cu–Mn ADI: A low cost high performance material. In: *Proceedings of 58th World Foundry Congress*, Poland; 1991.
- [12] Martins R, Moura P, Seabra J. MoS₂/Ti low-friction coating for gears. *Tribology International* 2006;39:1686–97.